



Contents lists available at ScienceDirect

Resources, Conservation & Recycling

journal homepage: www.sciencedirect.com/journal/resources-conservation-and-recycling

Full length article

Stability assessment of layer-by-layer nanofiltration membranes for element recovery from highly acidic media

Meret Amrein^{a,b,†}, Karina Rohrer^{a,†}, Dirk Hengevoss^a, Tobias Müller^a, Bastien Vallat^a, Dalila Rocco^a, Michael Thomann^a, Frank Nüesch^{b,c}, Sebastian Hedwig^{a,*}, Markus Lenz^{a,d}^a Institute for Ecopreneurship, School of Life Sciences, University of Applied Sciences and Arts North-western Switzerland, Hofackerstrasse 30, 4132 Muttenz, Switzerland^b EPFL, Institute of Materials Science and Engineering, Ecole Polytechnique Fédérale de Lausanne, Station 12, Lausanne 1015, Switzerland^c Empa, Swiss Federal Laboratories for Materials Science and Technology, Laboratory for Functional Polymers, Dübendorf 8600, Switzerland^d Department of Environmental Technology, Wageningen University & Research, P.O. Box 17 6700 AA, Wageningen, Netherlands

ARTICLE INFO

Keywords:

Thin-film photovoltaics
Critical raw materials
Element recovery
Hydrometallurgy
Circular economy
Life cycle assessment
Recycling

ABSTRACT

The recovery of critical raw materials such as indium (In) and silver (Ag) from end-of-life thin-film photovoltaics is essential for supporting the growing demand for renewable energy technologies. This study evaluates the acid stability of layer-by-layer nanofiltration (LbL-NF) membranes for metal recovery from acidic leachates to identify a sustainable alternative to conventional methods. Among various configurations, sPES(PAH/PSS)_n membranes exhibited outstanding resistance and long-term stability (> 300 h) in 5 % HNO₃, which potentially enables the recovery of 9100 g In and 6600 g Ag per m² of membrane. A life cycle assessment indicated a 34 %–46 % reduction in the global warming potential (GWP) of recycled Ag and a 40 %–50 % reduction for recycled In compared with the supply mix under modelled conditions. For Ag, the GWP was 137 g and 123 g CO₂-eq/g at 70 % and 80 % LbL-NF permeate recovery, respectively. For In, the GWP was 50 g and 55 g CO₂-eq/g at 70 % and 80 % recovery, respectively. These results highlight the climate benefits of LbL-NF membranes in circular resource recovery from end-of-life photovoltaics, which helps to identify key hotspots for optimisation and scale-up.

1. Introduction

The demand for efficient renewable energy technologies is high, and production is expected to increase. (Overview and key findings – World Energy Investment 2024) All renewable energy technologies rely on raw materials, rendering a functioning supply chain crucial for reaching climate change goals. (Directorate-General for Internal Market 2023; Lundaev et al., 2023) Moreover, some raw materials (e.g., lithium, cobalt, silicon and rare-earth elements) (Pommeret et al., 2022; Yu et al., 2023; Binnemans et al., 2015; Bae and Kim, 2021) are concurrently used in various other industrial applications, and their demand is expected to exceed primary production. (Schmidt et al., 2019; Rizos et al., 2024) The supply of raw materials in the European Union (EU) has been assessed under the Raw Material Initiative since 2008. Materials with an above-average economic importance and high supply risk are considered critical raw materials (CRMs). (Directorate-General for Internal Market 2023; European Innovation Partnership on Raw Materials. Raw Materials Scoreboard 2021) CRMs often represent limiting factors for

specific applications and sectors. (Pommeret et al., 2022) Hence, efficient low-cost recycling strategies for (critical) raw materials from end-of-life products will be essential to secure CRM supply and technological development in the future. (Lundaev et al., 2023) In response, the European Commission has issued the 2023 Critical Raw Materials Act, which dictates the recycling of at least 25 % of strategic raw materials (i.e., CRMs plus additional elements of strategic importance) (Directorate-General for Internal Market 2023).

This study focuses on the recycling of indium (In) and silver (Ag). Ag is used in electrodes for ‘conventional’ (silicon) photovoltaics as well as thin-film photovoltaics (TFPV). Due to its outstanding electric conductivity and electronic properties, Ag is used as an electrode material in highly efficient electronic products, the demand for which, along with TFPV, is expected to increase. (Lundaev et al., 2023; Newman et al., 2021) In is also used in electrode materials of TFPV, as well as in touchscreens and flatscreen monitors. (Park et al., 2023; Zhang et al., 2021) For both elements, there is competition for different end uses, which makes it challenging to predict future supply and demand.

* Corresponding author.

E-mail address: Sebastian.Hedwig@fhnw.ch (S. Hedwig).

† Shared first authorship.

<https://doi.org/10.1016/j.resconrec.2025.108630>

Received 16 March 2025; Received in revised form 26 September 2025; Accepted 6 October 2025

Available online 14 October 2025

0921-3449/© 2025 The Authors. Published by Elsevier B.V. This is an open access article under the CC BY license (<http://creativecommons.org/licenses/by/4.0/>).

(Lundaev et al., 2023; Schmidt et al., 2019; Zhang et al., 2021) With photovoltaic (PV) energy representing one of the cheapest energy sources available and driving the clean energy transition, (Renewables 2024) the demand for both elements will certainly increase in the years to come. Among the different TFPV technologies, ‘perovskite’ PVs in particular are expected to grow strongly in market share in the upcoming years. (Case et al., 2019; Li et al., 2020) The time point at which the demand for the two raw materials will actually exceed primary production has been the focus of several studies, (Wagner et al., 2023; Goldschmidt et al., 2021; Sverdrup et al., 2024; Apergis and Apergis, 2019; Click et al., 2024) although predictions remain difficult due to the complexity of the problem and various technical, economic, social, geological and geopolitical factors.

One direct measure to decrease supply risk is through recovering materials through recycling. In the EU, the current end-of-life (EOL) recycling rates (RR) of In and Ag are still low. While In is hardly recycled on an industrial scale (EOL RR = 0 %), Ag recycling is already established on a larger scale (EOL RR = 55 %). (European Innovation Partnership on Raw Materials. Raw Materials Scoreboard 2021) However, the contribution of Ag recycling to material need (i.e., the so-called ‘EOL recycling input rate’) is considerably lower (~19 %). Thus, for both elements, improved recycling strategies are urgently needed.

Different options for metal recovery exist, and pyro- and hydrometallurgical processes are well established on an industrial scale for most metals. Hydrometallurgical processes have shown high flexibility while having lower energy impact than high-temperature pyrometallurgical processes. (Zheng et al., 2023; Mejias et al., 2023) In hydrometallurgy, metals are commonly dissolved in aqueous media and purified (e.g., by solvent extraction or ion exchange). (Free, 2022) In contrast, the separation principle of nanofiltration (NF) is based on size and ion selectivity and therefore fundamentally different from classical hydrometallurgy. (Yaroshchuk et al., 2019) In NF membranes, the presence of a charged active layer causes electrostatic repulsion, which enhances the retention of multivalent ions (such as Mg^{2+} or In^{3+}) while allowing monovalent ions (such as Ag^+) and uncharged species, including non-dissociated acids and impurities, to permeate through the membrane. (Amrein et al., 2025) NF has gained increasing interest in the treatment of various acidic waste streams, as it can complement classical hydrometallurgy and thereby contribute to circular hydrometallurgy. (Botelho Junior et al., 2023; Hedwig et al., 2022; Zimmermann et al., 2014)

Conventional thin-film composite (TFC) NF membranes typically feature polyamide active layers, which lack stability in highly acidic environments ($pH < 2$). To address this limitation, alternative materials, such as polyamines, polyureas and polysulfonamides, have been developed for improved acid resistance. (G. Bargeman, 2021)

However, commercially available acid-resistant NF membranes often suffer from low permeability and require high operating pressure (20–40 bar), especially when operated in highly saline conditions. (Hedwig et al., 2022; Chen et al., 2023) Thus, the required electricity consumption of NF can be substantial, jeopardising the (economic) viability of its implementation. (Park et al., 2017) In contrast, layer-by-layer (LbL) NF membranes represent a promising low-cost alternative, as they are known to exhibit high permeability and require low transmembrane pressure (TMP) at comparable separation performance. (Scheepers et al., 2024) It has been shown that due to low TMP and high permeability, energy consumption could be considerably reduced when using LbL membranes instead of conventional NF membranes. (K. Remmen et al., 2019; Amrein et al., 2025) LbL membranes are produced by deposition of alternately charged polyelectrolyte (PE) layers on an ultrafiltration (UF) membrane substrate. (K. Remmen et al., 2019) Thus, LbL membranes offer the opportunity to alter separation performance by changing the type of PE, the amount of PE bi-layers (BL) and the coating conditions (e.g., salt concentration in the coating solution). (Paltrinieri et al., 2019; Yu et al., 2024) Overall, LbL membranes are a promising technology for future NF applications. However, they are known to

suffer from instability when used in highly saline or strong acidic solutions. (Chen et al., 2023; Lee et al., 2023; Remmen et al., 2020) As extractive hydrometallurgy commonly relies on acidic media and/or concentrated solutions, LbL membrane stability remains a crucial challenge for large-scale application in this field. (Jonkers et al., 2023; Botelho Junior et al., 2023)

Therefore, this study systematically analyses the stability of LbL membranes in various highly concentrated inorganic acids (hydrochloric, sulfuric, phosphoric and nitric acid). The primary objective is to identify LbL membranes capable of withstanding concentrated acidic solutions as typically used in hydrometallurgical processing. To achieve this, the filtration performance of LbL membranes with different configurations was evaluated before and after acid exposure through magnesium (Mg^{2+}) retention and permeate flux. One of the membranes showing partial resistance to the harshest conditions was subjected to an equimolar saline solution, shedding light on possible degradation mechanisms. Subsequently, the most stable membrane was tested for the recovery of In and Ag from highly acidic (5 % HNO_3) EOL TFPV leachates in a long-term (300 h) filtration experiment. In addition, this study assesses the environmental performance of the recovery approach. A life-cycle assessment compared the environmental impacts of LbL-based recycling with those of primary mining.

2. Methods

2.1. Chemicals and materials

For acid stability experiments, HNO_3 (67 %, trace metals grade, Sigma-Aldrich, Basel, Switzerland), HCl (32 %, semiconductor grade, Honeywell, Basel, Switzerland), H_2SO_4 (95 %–97 %, ACS, ISO, Reag. pH Eur, Sigma Aldrich, Basel, Switzerland) and H_3PO_4 (85 wt % in H_2O , 99.99 % trace metals basis) were diluted in nanopure water to obtain a concentration of 10 wt % for each solution.

2.2. Analytical methods

All metal analyses were performed on a 5800 ICP-OES system (Agilent, Basel, Switzerland) using general-purpose operational settings. Quantification was performed via external calibration with multi-element standards using Mg (279.800 nm), Ag (328.068 nm) and In (230.606 nm). Y (371.029 nm) was used as an internal standard to account for the matrix effects. All elements were measured in axial and radial modes.

2.3. Membrane support

Polyethersulfone (PES) and sulfonated polyethersulfone (sPES)-based hollow fibre membranes provided by Pentair (Enschede, Netherlands) were used as a support structure to prepare LbL membranes (see Section 2.4). The PES membrane had a molecular weight cut-off of 100 kDa and a pure water permeance of $1100 \text{ L m}^{-2} \text{ h}^{-1} \text{ bar}^{-1}$, while the sPES membrane had a cut-off of 10 kDa and a pure water permeance of $80 \text{ L m}^{-2} \text{ h}^{-1} \text{ bar}^{-1}$. The membranes were potted in modules containing one fibre each. Each hollow fibre had an inner diameter of 0.8 mm and a length of 300 mm. This resulted in a total membrane surface of 7.5 cm^2 per module. After potting, the uncoated membranes were immersed in deionised water overnight.

2.4. Layer-by-layer membrane modification

Coating of the UF membrane substrate with polyelectrolytes (PEs) was carried out dynamically using a custom-made set-up in which dead-end filtration was applied to concentrate the PE inside the lumen of the membrane. (K. Remmen et al., 2019) The positively charged PE was either poly(diallyldimethylammonium) chloride (PDADMAC; MW = 400–500 kDa, 20 % in water) or polyallylamine (PAH; MW = 65 kDa, 10

wt % in water). The negatively charged PE was poly(sodium styrenesulfonate) (PSS; MW = 1000 kDa, 25 wt % in water). All chemicals were purchased from Sigma-Aldrich (Buchs, Switzerland). The oppositely charged PEs were diluted in a NaCl solution (0.5 M) and alternately coated onto the membrane, starting with the positively charged PE and always terminated with PSS. The pH of the coating solution was neutral. After each coating cycle, the membrane was flushed with deionised water until conductivity below $7 \mu\text{S cm}^{-1}$ was reached. The conductivity was measured using a GMH 3451 conductivity meter (Greisinger, Regenstauf, Germany).

2.5. Membrane filtration

A custom-made testing device was used for filtration (Figure S1). At a TMP of 5 bar, a BVP-Z gear pump (Ismatec, Switzerland) was used to establish the desired crossflow velocity for operation in turbulent mode. Experiments were performed in batch circulation mode, with the concentrate fed back into the feed vessel. Elemental retention was determined in cross-flow mode. At a TMP of 5 bar, the flow rate was 90 mL min^{-1} (cross-flow velocity = 2.65 m s^{-1}), resulting in a turbulent flow (Reynolds number > 2300). Each LbL membrane modification was performed in triplicate. Experiments were performed at room temperature.

Ion concentrations in the permeate and the retentate were used to calculate the retention value (Equation S1). (K. Remmen et al., 2019) The permeate flux was determined as the collected permeate volume over time and indicated in $\text{L m}^{-2} \text{ h}^{-1}$ (LMH, Equation S3). The permeance was calculated as the permeate flux normalised by the applied pressure (equation S4).

2.6. Feed solutions

Mg retention was determined using a MgSO_4 feed solution (0.05 M). $\text{MgSO}_4 \cdot 7 \text{ H}_2\text{O}$ ($\geq 99\%$, p.a. ACS) was dissolved in nanopure water. The pH of the feed solution was neutral. Long-term acid resistance filtration and permeate recovery experiments were performed using a model solution based on an acidic perovskite solar cell (PSC) extraction composition. $\text{In}(\text{NO}_3)_3 \times \text{H}_2\text{O}$ (99.99 % trace metal basis, Sigma-Aldrich, Switzerland) and AgNO_3 (99.99 % trace metal basis, Sigma-Aldrich, Switzerland) were dissolved in HNO_3 (5 % w/w) targeting final concentrations of 1 g/L for both Ag and In.

2.7. LbL stability experiments

Stability experiments of LbL membranes were conducted as follows: First, membrane filtration experiments (described in Section 2.5) were conducted to determine Mg^{2+} retention and permeate flux of untreated membranes. Subsequently, LbL membranes were immersed in 10 % HCl, 10 % HNO_3 , 10 % H_2SO_4 and 10 % H_3PO_4 , respectively, for 15 h. After acid exposure, LbL membranes were rinsed with nanopure water for at least 20 min before membrane filtration experiments were conducted again to determine Mg^{2+} retention and permeate flux of acid-treated membranes. All membranes were tested in triplicate.

2.8. Element recovery filtration experiments

Before filtration, the membranes were rinsed with deionised water for 20 min. When the filtration was run in continuous filtration mode, the permeate flowed back into the feed tank and the retentate was therefore not concentrated over time. In contrast, the permeate was collected during the permeate recovery experiments. The permeate recovery was calculated as the ratio of the collected permeate to the initial feed volume (Equation S2). Filtration tests were performed until a permeate recovery of 70 % was reached. Samples were taken after every 10 % of permeate recovery.

2.9. Life cycle assessment analysis

A life cycle assessment (LCA) was conducted to identify the environmental hot spots of the In and Ag recovery processes (as $\text{In}(\text{OH})_3$ and AgCl) presented in this study and to compare their environmental impacts with those of primary In and Ag production and other recycling alternatives reported in the literature. The LCA followed ISO 14,040:2006 standard guidelines (ISO 2025) and was performed using SimaPro software (version 9.6.0.1) combined with the Ecoinvent (version 3.10) database. The global warming potential over 100 years (GWP100) was calculated using the IPCC 2021 method and expressed in $\text{gCO}_2\text{-eq.}$ (Intergovernmental Panel On Climate Change (ipcc) 2023) The functional unit was 1 g of recovered In or Ag. The environmental footprint (EF) method was used for sensitivity mainly to demonstrate the correlation of GWP with other environmental impacts. (European Commission 2023) Other sensitivity analyses examined key assumptions such as microfiltration (MF) membrane lifetime (MLT) and permeate recovery rates of 70 % or 80 % in the LbL-NF step, resulting in an overall recovery rate of 60 %–69 % for Ag and 84 % for In (Hawach Scientific 2024) The LbL-NF permeate recovery was based on experimental values (70 %) and modelled at a higher recovery of 80 % to show potential benefit from improved performance at the industrial scale. The lifetime of the LbL membrane was set to 300 h, as assessed experimentally. Two membrane lifetime scenarios (MLT1 = 300 h and MLT2 = 3 months) were assumed for the MF membranes used for solid–liquid separation.

The impact along the recycling process was allocated among the different outputs based on economic value (Fig. 1 and Table S1). The life cycle inventory (LCI) was expanded based on the process flow chart in Fig. 1. More details on the LCA definitions, LCI and life cycle impact assessment can be found in the supplementary information (Section S2).

3. Results

3.1. Membrane stability screening

The stability of the LbL membranes against different mineral acids was determined from the change of Mg^{2+} retention and permeate flux after 15 h of acid exposure to the respective acids (Fig. 2, Table S3). Thus, the LbL membrane stability was divided into three categories. Membranes with a change in Mg^{2+} retention of ± 0.1 were defined as stable and membranes with a change of Mg^{2+} retention of >0.3 were defined as unstable. Membranes with a change of Mg^{2+} retention between 0.1 and 0.3 were defined as metastable (i.e., showing some signs of degradation). Consequently, some membranes that showed stable retention (<0.1) but a substantial increase in flux (>10 LMH) were also classified as metastable.

Clear tendencies could be observed concerning the acid stability of different LbL membrane compositions (including the UF substrate and PE combinations) as well as the effect of the tested acids. It was observed that sPES-based LbL membranes generally exhibited higher stability than PES-based membranes (Fig. 2, Table S3). As such, only up to a 0.3 drop in Mg^{2+} retention was observed for sPES, whereas the highest Mg^{2+} retention drop for PES-based membranes was 0.46. Similarly, sPES-based membranes showed only a moderate increase in flux (up to 16 LMH relative to the initial flux), whereas the strongest increase in flux of PES-based membranes was sizably higher (131 LMH of initial; Fig. 2). Furthermore, LbL membranes using polycation PAH were considerably more stable than LbL membranes using polycation PDADMAC. In these experiments, unstable membranes were observed only for PES(PAH/PSS)₄, which was immersed in HCl. In contrast, membrane instability was observed for all membranes using PDADMAC, which were immersed in HCl and HNO_3 . Overall, the sPES(PAH/PSS)₄ membrane showed the highest stability in all tested acids, as the change in Mg^{2+} retention and flux was the least pronounced in the current experiments for sPES(PAH/PSS)₄. In contrast, the strongest change in retention and flux was observed when using a PES(PDADMAC/PSS)₆ membrane.

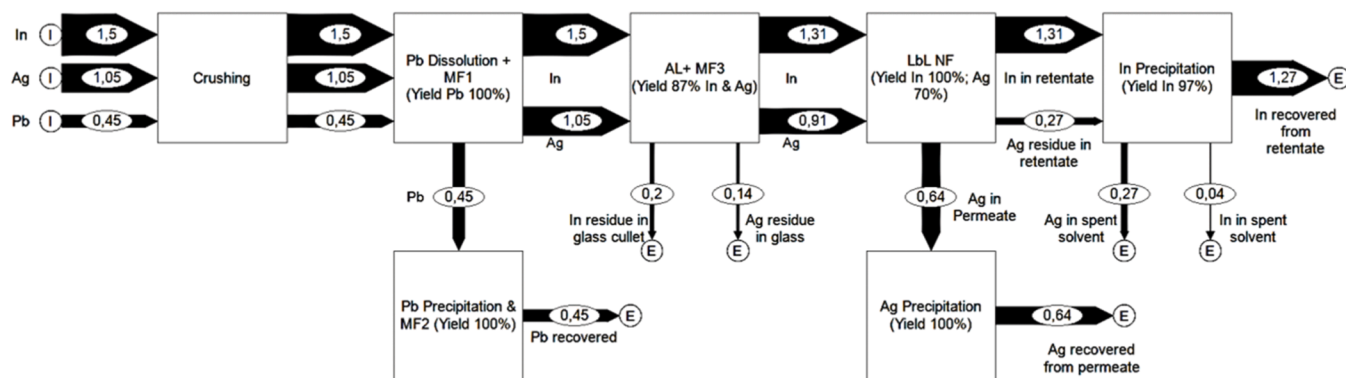


Fig. 1. Flowchart of the recycling process steps showing the mass change of In, Ag and Pb in grams recovered from 1 m² of TFPV along the recycling process at prospective recovery rates of 70 % Ag and 97 % in LbL-NF. MFx: microfiltration step x; AL: acid leaching; LbL-NF: layer-by-layer nanofiltration. The overall recovery rate of the recycling process, therefore, is 60 % for Ag and 84 % for In. Only elemental yields and masses are considered in this figure; however, the metals are recovered in the form of In(OH)₃ and AgCl, which require additional refining to obtain pure elements. (Zheng et al., 2023; Oliveira et al., 2020).

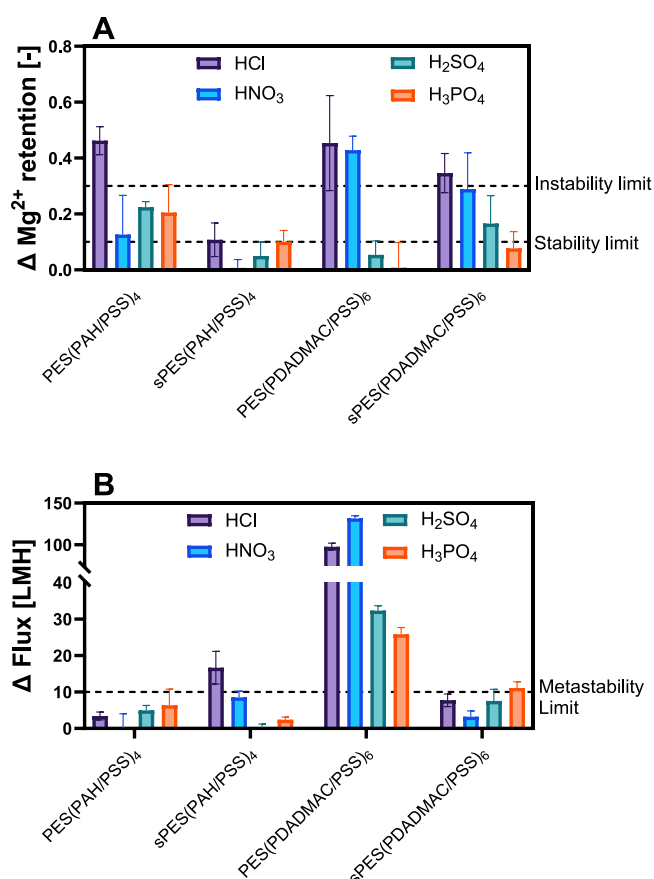


Fig. 2. Difference of Mg²⁺ retention (A) and permeate flux (B) before and after acid exposure for all tested LbL membranes and acids. The limits for membrane stability, metastability and instability are marked in the graphs.

Regarding the type of acid, the highest impact on stability was observed after immersion in 10 % HCl, where membrane instability was observed for all tested membranes except sPES(PAH/PSS)₄, which was classified as metastable. A considerably higher stability was observed for all other acids. In addition, HNO₃ exposure resulted in stronger membrane instability when using PES(PDADMAC/PSS)₆, while the other membranes showed similar stability towards HNO₃, H₂SO₄ and H₃PO₄. In summary, the following tendencies have been observed for the stability of LbL membranes using pre-filtration exposure to different acids:

- sPES > PES
- PAH > PDADMAC
- H₃PO₄ ≈ H₂SO₄ > HNO₃ > HCl

3.2. Effect of salinity on LbL membrane stability

Immersion of a PES(PAH/PSS)₄ membrane in 2.87 M NaCl (corresponding to the chloride concentration of 10 wt % HCl) resulted in a considerable decrease in Mg²⁺ retention from 0.81 ± 0.05 before to 0.57 ± 0.07 after NaCl immersion (Table S4). At the same time, the flux increased substantially from 32.0 ± 0.3 to 52 ± 2 LMH. However, the retention drop was smaller compared with immersion in 10 % HCl, where Mg²⁺ retention decreased from 0.88 ± 0.01 before to 0.42 ± 0.05 after HCl immersion.

3.3. Element recovery by LbL membrane filtration

As sPES(PAH/PSS)₄ was determined to be the most stable of the tested LbL membranes, its long-term stability was evaluated in a model solution containing 5 wt % HNO₃ and 1 g/L each of In and Ag (present as ionic In³⁺ and Ag⁺). (Amrein et al., 2025) When operated in continuous filtration mode (i.e., returning the permeate to the feed tank), In³⁺ and Ag⁺ retention remained stable (0.96 ± 0.03 for In³⁺ and 0.0 ± 0.1 for Ag⁺) over >300 h of filtration (Fig. 3).

Additionally, In³⁺ retention (0.991 ± 0.001 in both the first and second filtrations) and Ag⁺ retention (0.02 ± 0.03 in the first filtration and 0.00 ± 0.03 in the second filtration) remained stable over 70 % permeate recovery (Fig. 4). Within the standard deviation range, the permeate fluxes during both filtrations were similar (22 ± 1 LMH in each case; Fig. 4C), although a slightly steeper decline towards the end of the second filtration was noted.

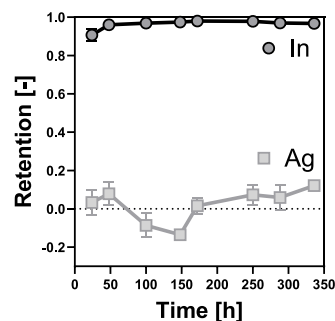


Fig. 3. Long-term (300 h) In and Ag retention (5 % HNO₃, pH 0) of a sPES (PAH/PSS)₄ LbL membrane.

3.4. Life cycle impact assessment (LCIA)

3.4.1. Environmental impacts of In and Ag

In the first scenario (MLT1; MF membrane lifetime of 300 h, matching LbL stability; Fig. 3, Table 1), the GWP100 for In was 60 g and 55 g CO₂-eq/g at 70 % and 80 % permeate recovery, respectively. For Ag, the GWP100 was 137 g and 123 g CO₂-eq/g at 70 % and 80 % recovery, respectively.

In the second scenario (MLT2; MF membrane lifetime of 3 months; Table 2), the GWP100 for In was 58 g and 54 g CO₂-eq/g at 70 % and 80 % permeate recovery, respectively. For Ag, the corresponding values were 132 g CO₂-eq/g and 121 g CO₂-eq/g.

3.4.2. By-products

For Pb, the LbL-NF process achieved a GWP100 of 1.20×10^{-1} and 1.17×10^{-1} g CO₂-eq/g for MLT1 and MLT2, respectively. Glass cullet recovery (glass mixture containing 13 % of total Ag and In) showed negligible contributions, ranging from 1.14×10^{-2} to 1.29×10^{-2} g CO₂-eq/g depending on the permeate recovery and MLT scenario.

4. Discussion

4.1. Design of acid-stable LbL membranes

Among the tested membranes, sPES(PAH/PSS)₄ showed the highest stability across all acids. It was the only membrane to maintain high stability in HNO₃, whereas others (e.g., PES(PAH/PSS)₄) exhibited a <0.12 reduction in Mg²⁺ retention. After exposure to H₂SO₄ or H₃PO₄, most membranes showed only minor retention decreases, but sPES (PAH/PSS)₄ uniquely maintained permeate flux. In HCl, Mg²⁺ retention dropped by only 0.10, confirming its exceptional acid resistance.

Compared with thin-film composite (TFC) NF membranes tested under similar acidic conditions (Yin et al., 2025; Lasisi et al., 2025) (Table S5), sPES(PAH/PSS)₄ showed superior retention stability. For example, after HNO₃ exposure, Yin et al. reported a 7 % decrease in Mg²⁺ retention and ~40 % increase in permeance (Table S5), (Yin et al., 2025) while the sPES(PAH/PSS)₄ membrane experienced only a ~1 % retention loss and a ~38 % permeance increase (Table S3). Lasisi et al. observed minimal retention changes in a PSF/b-PEI/CC TFC membrane but with a 13 % permeance increase (Table S5). (Lasisi et al., 2025) Both TFC membranes had higher permeabilities (2.2 times and 6 times that of sPES(PAH/PSS)₄). (Yin et al., 2025; Lasisi et al., 2025)

The PE pair PAH/PSS was generally more acid-stable than PDAD-MAC/PSS (Fig. 2, Table S3), likely due to higher intermolecular binding strength. (J. Fu et al., 2017) Aside from the PE type, the sPES-based LbL

Table 1

LCIA results (EF score and GWP100) per gram of material output under the MLT1 scenario, comparing LbL-NF permeate recovery yields (70 % vs 80 %).

Material	LbL-NF Permeate Recovery	70 %		80 %		
		Total Yield	GWP 100 [g CO ₂ -eq/g]	EF [μPt/g]	GWP 100 [g CO ₂ -eq/g]	EF [μPt/g]
Ag	60 %–69 %		1.37×10^2	1.21×10^1	1.23×10^2	1.09×10^1
In	84 %		5.95×10^1	5.17×10^0	5.55×10^1	4.76×10^0
Pb	100 %		1.20×10^{-1}	1.07×10^{-2}	1.20×10^{-1}	1.07×10^{-2}
GC	100 %		1.29×10^{-2}	1.14×10^{-3}	1.16×10^{-2}	1.02×10^{-3}

MLT1: Microfiltration and LbL membrane lifetime of 300 h. The LbL-NF permeate recovery directly influences the Ag yield and indirectly affects the impacts of In and GC through allocation changes. Climate change accounted for ~30 % of total EF impacts, followed by fossil resource use (~30 %).

Table 2

LCIA results (EF score and GWP100) per gram of material output under the MLT2 scenario, comparing LbL-NF permeate recovery yields (70 % vs 80 %).

Material	LbL-NF Permeate Recovery	70 %		80 %		
		Total Yield	GWP 100 [g CO ₂ -eq/g]	EF [μPt/g]	GWP 100 [g CO ₂ -eq/g]	EF [μPt/g]
Ag	60 %–69 %		1.32×10^2	1.16×10^1	1.21×10^2	1.07×10^1
In	84 %		5.80×10^1	4.98×10^0	5.40×10^1	4.68×10^0
Pb	100 %		1.17×10^{-1}	1.04×10^{-2}	1.17×10^{-1}	1.04×10^{-2}
GC	100 %		1.26×10^{-2}	1.11×10^{-3}	1.14×10^{-2}	1.00×10^{-3}

MLT2: Microfiltration membrane lifetime of 3 months (2160 h),⁴⁵ LbL membrane lifetime of 300 h; GC: glass cullets. The LbL-NF permeate recovery directly influences the Ag yield and indirectly affects the impacts of In and GC through allocation changes. Climate change accounted for ~30 % of total EF impacts, followed by fossil resource use (~33 %).

membranes were generally more acid stable than those based on PES. Hence, Mg²⁺ retention dropped more for PES-based membranes compared to those made of sPES. Here, most likely, sulfonation substantially improved the binding forces of sPES to polycations (and thus PEs) by creating a strongly negatively charged membrane surface. (de

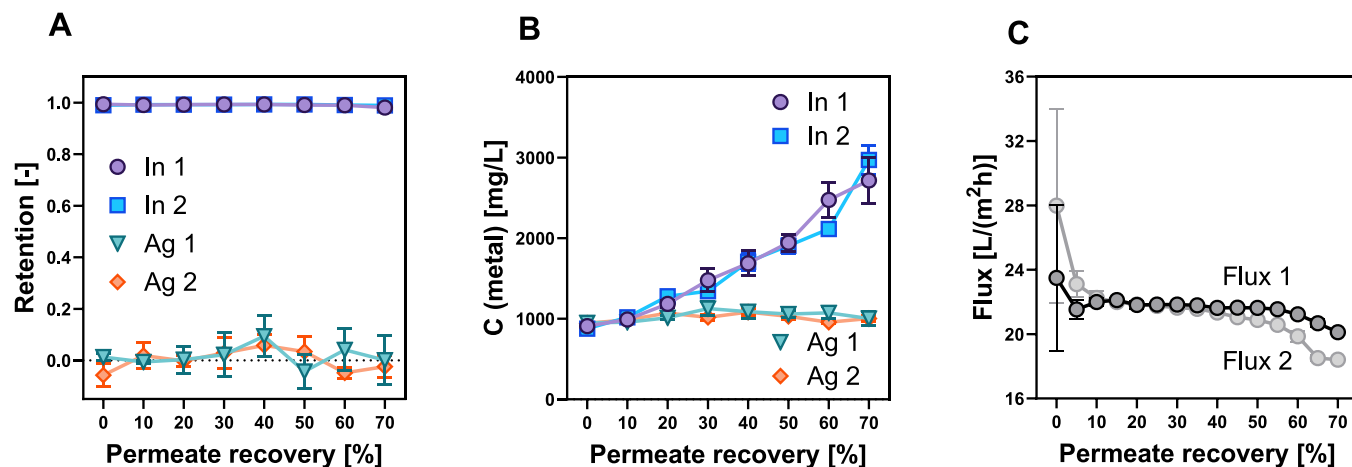


Fig. 4. Comparison of the retention (A), metal concentration (B) and flux (C) of a sPES(PAH/PSS)₄ LbL membrane over 70 % permeate recovery, where (1) shows the first recovery test and (2) the second one performed with the same membrane.

Grooth et al., 2015; M.G. Elshof et al., 2020) While sPES(PAH/PSS)₄ was the most stable membrane, PES(PDADMAC/PSS)₆ showed the highest stability loss.

Importantly, PAH forms stronger ionic interactions with PSS than PDADMAC, due to higher charge density and lower steric hindrance of the primary amine groups, resulting in enhanced membrane stability. (J. Fu et al., 2017) Previous studies have shown that PE complexes with stronger ion pairing (i.e., higher binding strength) are more resistant to swelling and delamination in harsh ionic environments. (Chen et al., 2023) Thereby, the strength of ion pairing can be quantified via the Gibbs free energy of polyelectrolyte association (ΔG_a°), which reflects the difference in binding strength between PAH/PSS ($\Delta G_a^\circ = -6.34$ kJ/mol) and PDADMAC/PSS ($\Delta G_a^\circ = -2.19$ kJ/mol). (J. Fu et al., 2017) Based on this, PE pairs with high ΔG_a° could result in highly acid-stable LbL membranes, suggesting that substitution of PAH with polyvinyl amine (PVA) could be an interesting option (ΔG_a° (PVA/PSS) = -7.10 kJ/mol). (J. Fu et al., 2017)

Furthermore, it has been shown that considerably lower polycation concentrations were required for comparable ion retention when using PE pairs with stronger ionic interaction. (Paltrinieri et al., 2019) Indeed, in this study, the amount of PAH used per coating layer (0.2 g/m²) was 10 times lower than the respective amount of PDADMAC (2 g/m²). Additionally, for (PAH/PSS)-based membranes, four BL were found sufficient for high Mg²⁺ retention, while at least six BL were necessary with the combination (PDADMAC/PSS) to achieve similar results. Hence, aside from the higher acid stability, using (PAH/PSS) allows for lower material requirements at higher retention.

LbL membranes are known to suffer from stability issues in acidic and saline solutions. The phenomenon commonly referred to as ‘doping’ (i.e., the breaking of ionic bonds between PE pairs) has been determined as the main instability mechanism of LbL membranes in highly saline solutions. (Fu and Schlenoff, 2016) Doping weakens intrinsic bonds (i.e., PE–PE), resulting in a looser LbL membrane structure and swelling, which is frequently reported. (Chen et al., 2023; Remmen et al., 2020) The doping rate depends on different factors. On the one hand, PE pairs with a higher binding strength (i.e., the Gibbs free energy of PE association) have shown higher resistance against doping. (J. Fu et al., 2017) On the other hand, it has been shown that the ability of ions to associate with PE charges could be characterised with the Hofmeister series, where chaotropic ions (e.g., Br⁻, SCN⁻, Cl⁻ or NO₃⁻) have a higher affinity for doping than kosmotropic ions (e.g., CO₃²⁻, SO₄²⁻ and S₂O₃²⁻). (O’Neal et al., 2018) Consequently, similar effects have been observed in acidic media, where swelling of the LbL coating layer and change in surface morphology have been observed, resulting in higher permeability of the membrane. (Remmen et al., 2020) Furthermore, differences in the stability of LbL membranes have been explained by differences in the electrostatic interactions between the PE. (M.G. Elshof et al., 2020) However, in-depth analyses of LbL stability in highly acidic environments have rarely been reported.

Based on the aforementioned observations, HNO₃ and HCl were expected to destabilise the PE coating the most, due to their chaotropic corresponding bases (NO₃⁻ and Cl⁻, respectively; Figure S2). (Chen et al., 2023) Indeed, Mg²⁺ retentions dropped the most after immersion in HCl or HNO₃ (Fig. 2, Table S3). Notably, the retention decreased more after HCl exposure, which was likely due to the higher molarity of 10 % HCl (2.87 mol/L vs 1.67 mol/L for 10 % HNO₃). In contrast, under the current conditions H₃PO₄ (10 % and 1.08 mol/L) and H₂SO₄ (10 % and 1.09 mol/L) were largely present as neutral H₃PO₄ and monovalent HSO₄⁻, which have a lower affinity to interpenetrate the PE bi-layers and compensate the PE charges extrinsically. Additionally, H₂PO₄⁻ and SO₄²⁻ were expected to occur at lower concentrations (Figure S2), and both were more kosmotropic than NO₃⁻ and Cl⁻, resulting in a weaker doping effect. (Chen et al., 2023) Indeed, after exposure to phosphoric and sulfuric acid, the stability was still high for all LbL membranes.

This experiment mainly considered anions, as previous studies have usually reported stronger doping effects for these than for cations.

(O’Neal et al., 2018) However, H⁺ ions might have additional effects on membrane stability, such as the protonation of the anionic sulfonate moieties of PSS. The sulfonic acid groups of PSS have a pK_A of 1; therefore, protonation of the sulfonate may occur at a very low pH (as in this study). (PDF 2022) To quantify the destabilising effect of cations compared to protons, Mg²⁺ retention was measured before and after immersion of a PES(PAH/PSS)₄ membrane in 2.87 M NaCl and compared to HCl exposure (Table S4). Likewise, a considerable decrease in Mg²⁺ retention was observed after NaCl exposure, indicating the strong doping effect of Cl⁻ anions. However, the decrease in retention after HCl immersion was greater, likely due to the protonation of PSS by free H⁺.

In summary, the factors affecting LbL membrane stability can be predicted with theoretical assumptions. However, the current work identified general trends rather than statistically significant differences. Further research is needed to increase the statistical robustness of the findings. Furthermore, the current work aligns with previously reported studies. (K. Remmen et al., 2019; Paltrinieri et al., 2019; Remmen et al., 2020; G. Bargeman, 2021) As found in this study, significant stability issues have already been reported when applying LbL membranes for the filtration of HCl waste streams. (K. Remmen et al., 2019) Thus, strong dilution and neutralisation of the feed solutions were necessary to allow stable filtration. Hence, commercial acid-resistant NF membranes might be better suited for the filtration of HCl (waste) streams. (Hedwig et al., 2022; S. Hedwig et al., 2023) In contrast, highly stable LbL membranes for the application in H₃PO₄ waste streams have been reported. (Remmen et al., 2020) These results indicate that considering the feed matrix is crucial for the application of LbL membranes.

4.2. Application of highly stable LbL-NF membranes for In and Ag recovery from EOL PSC

The current study follows up on previous work in which a proof-of-concept recycling process for In and Ag from EOL perovskite solar cells (PSC) was developed using acidic extraction with HNO₃ and LbL NF. (Amrein et al., 2025) HNO₃ has been frequently reported as a matrix in hydrometallurgical processes for both In and Ag. (Fthenakis et al., 2020; Savvilotidou and Gidaracos, 2020) The combination of high oxidation potential and strong acidity facilitates fast leaching kinetics using HNO₃. One main advantage of HNO₃ compared to other inorganic acids is its ability to dissolve metals efficiently. (Oliveira et al., 2020; Fthenakis et al., 2020) Particularly for the extraction of Ag, HNO₃ is one of the few choices due to its formation of soluble silver nitrate (AgNO₃) instead of poorly soluble salts like AgCl. (Oliveira et al., 2020) Hence, the stability of the LbL membrane in HNO₃ is of particular interest. In this study, the most stable LbL membrane in HNO₃ had the configuration sPES(PAH/PSS)₄ and was therefore selected for long-term filtration experiments.

All long-term filtration experiments have confirmed the high stability of sPES(PAH/PSS)₄ over the entire filtration period (> 300 h). When running the filtration in continuous mode (i.e., recirculating the permeate and without concentrating the feed), In³⁺ and Ag⁺ retentions were stable for >300 h (0.96 ± 0.03 for In³⁺ and 0.0 ± 0.1 for Ag⁺). Even at the termination of the experiment, no signs of degradation were observed based on In³⁺ and Ag⁺ retentions (Fig. 3). Hence, a lifetime of 300 h can be assumed as a minimum and even longer filtration times should be possible in practice.

Furthermore, in the permeate recovery experiments, the same membrane was used to concentrate (70 % permeate recovery) two batches of HNO₃ (5 wt %) containing In³⁺ and Ag⁺. Stable retentions of In³⁺ and Ag⁺ were observed (Fig. 4A). Ag⁺ was virtually not retained, resulting in no considerable change in its concentration in the retentate (Fig. 4B). In contrast, In³⁺ was almost completely retained, leading to a 3.3 times increase in its concentration (Fig. 4B). These results further underline the stability of the sPES(PAH/PSS)₄ membrane in HNO₃, and its selectivity for multivalent over monovalent ions remains virtually

unchanged. The permeate fluxes during both filtrations were similar (Fig. 4C). As changes in neither the retentions of In^{3+} and Ag^+ nor in the permeate fluxes were observed during the second filtration, membrane fouling or scaling either did not occur or was negligible under the tested conditions. Collectively, these results confirm the reusability and stable separation performance of the sPES(PAH/PSS)₄ membrane in HNO_3 during repeated batch operations. As permeate fluxes remained high after 70 % recovery, future work could explore greater concentrations by minimising system dead volume and increasing membrane area to boost permeate generation.

Permeate fluxes remained high beyond 70 % recovery, indicating that further concentration could be explored in future work. In the present study, however, concentration was limited by the experimental design, which required sufficient volume for turbulent cross-flow and stepwise sampling; with larger feed volumes and endpoint sampling, higher concentration would have been possible.

Considering a minimal LbL membrane lifetime of 300 h and measured permeate fluxes (22 LMH), a recovery of at least 6600 L permeate/m² membrane area could be possible. At a 70 % permeate recovery rate, this would translate into the recovery of approximately 9100 g In and 6600 g Ag before a membrane replacement would be needed (for yields, see Fig. 1).

A key finding from the LCA was the identification of electricity consumption as the predominant environmental impact of the recycling process, accounting for approximately 75 %–85 % of the total GWP. The largest share (around 47 %) of this electricity demand resulted from acid leaching, which was modelled as a 24-hour process at 60 °C, with approximately 23 % attributed to stirring and 24 % attributed to heating. Crushing of the solar cells also accounted for around 40 %, while the remaining 13 % originated mostly from heating during lead extraction. The filtration steps consumed <1 % of total energy, making their impact negligible at the currently assumed recovery rates.

Compared to conventional NF, LbL-NF membranes in previous studies have achieved equivalent separation at substantially lower pressure (5 bar vs 30 bar), leading to reduced electricity use per volume treated. (Hedwig et al., 2022; S. Hedwig et al., 2023) Improving the efficiency of industrialised recycling and consequently reducing the GWP of the extracted metals could be achieved by (1) increasing permeate recovery through process optimisation, (2) using waste heat from other processes at leaching (in the LCA, electric heating was considered) and (3) using alternative approaches for separation of glass from the solar modules (if the panels have not been damaged) to eliminate the need for crushing. However, given that crushing is a well-established step in PV recycling facilities, replacing this technology presents challenges. (Fthenakis et al., 2020, Sinha et al., 2018) Thus, extending the lifetime of filtration membranes might be an option to reduce impact, particularly since membranes are expected to be incinerated at their end of life. (Szekely et al., 2014; Sustainability in Membrane Technology 2025)

With a focus on LbL membranes, this highlights the importance of finding a good trade-off between highly stable and highly permeable LbL membranes. Regarding the depicted scenario, an ideal candidate with sPES (sPES (PAH/PSS)₄) was found. Using alternatives to MF such as vacuum belt filtration, filter presses or centrifugation is more suitable for industrial scale production. (Rushton et al., 1996)

Although the electricity share of filtration was <1 % in the entire recycling process considering the context of the experimental set-up, the electricity consumption of industrial-scale membrane filtration can be substantially decreased, compared to bench-scale filtration, through optimised crossflow and design considerations. (S. Hedwig et al., 2023)

In the current process, LbL-NF separated In^{3+} and Ag^+ effectively, offering the permeate as a viable stream for reuse. Ag precipitation methods such as with HCl/NaCl or electro precipitation do not significantly alter the pH, enabling direct reuse of the permeate. (Oliveira et al., 2020; Savvilitidou and Gidarakos, 2020) In contrast, In is usually won by precipitation with NH_4OH , neutralising the HNO_3 and

impairing/preventing direct reuse. (Zheng et al., 2023) However, NF considerably concentrates In^{3+} in the retentate (more than threefold concentration, Fig. 4B) and separates 70 % of the original volume with the permeate. As a result, even if the retentate is lost by neutralisation, most of the acid could still be reused, which would influence the yield of Ag and reduce the GWP, as demonstrated in the sensitivity analysis. The most important aspect will be the balancing of recovery yields and energy/material consumption considering their environmental and economic consequences.

Considering the supply mix of Ag and In and alternative e-waste recycling approaches, Nuss and Eckelman (Nuss and Eckelman, 2014) reported a GWP of 196 g $\text{CO}_2\text{-eq g}^{-1}$ for Ag sourcing – approximately 30 %–37 % higher than that achieved through the LbL-based recycling process developed in this study. In addition, for In, the GWP was 102 g $\text{CO}_2\text{-eq/g}$, around 40 %–50 % higher than the GWP of the recycling process under the modelled process conditions. (Nuss and Eckelman, 2014) An impact analysis by Farjana et al. (Farjana et al., 2019) of Ag refining from established couple production of gold-silver from primary resources reported a GWP of 815 g $\text{CO}_2\text{-eq/g}$. This value is almost a factor 6 higher than the GWP of Ag recovered by the LbL membranes.

Luling et al. (Yu et al., 2019) reported the life cycle impacts of an experimental recycling process for EOL liquid crystal display (LCD) screens containing 326.98 mg In per kg of waste. The process involved crushing, hydrothermal treatment and acid leaching. Based on their reported GWP values – 6002 g $\text{CO}_2\text{-eq}$ and 9620 g $\text{CO}_2\text{-eq}$ per kg of treated LCD waste – and then applying economic allocation using the economic values considered in the present study, the resulting GWP per gram of recovered In amounts to 11,000 g $\text{CO}_2\text{-eq/g}$ and 17,700 g $\text{CO}_2\text{-eq/g}$, respectively. These values are approximately 220 and 354 times higher than those obtained for In recovery using the LbL membrane process in this study. The considerable difference appears to be primarily driven by higher reported electricity and chemical consumption in the experimental LCD recycling approach.

Even though there are variations in GWP compared to the literature, LCIA depends on model assumptions like flow inputs, outputs and allocation parameters, and whether these are derived from experimental/theoretical values. However, LbL-NF at high yields can be seen as a low-impact process step in recycling Ag and In from EOL TFPV. Finally, while GWP accounts for approximately 30 % of the total environmental footprint, (European Platform on LCA | EPLCA 2025) it does not capture all relevant impact categories. Midpoints such as resource depletion accounting for around 33 % of total EF should also be considered, particularly as the supply criticality of In and Ag may increase substantially in the coming decades. From this perspective, low-impact recycling will become even more important for reducing overall environmental footprint and remains a key strategy for improving the long-term sustainability of photovoltaic supply chains.

4.3. Further implications

The European Green Deal aims to reach climate neutrality by 2050 as the promotion of renewable energy sources continues to grow. (Fetting, 2020) At the same time, the demand for raw materials and rare metals will remain high, and the criticality of those used in clean technologies may increase. (Pommeret et al., 2022) In and Ag may limit the deployment for TFPV, particularly with perovskites on the rise. (Wagner et al., 2023) Their recycling from EOL PSC will also be important from a regulative perspective. (Directorate-General for Internal Market 2023; Lundaev et al., 2023) To date, recycling rates of most CRMs are low, especially since recycling is often not economically feasible and chemical use is high. (Rizos et al., 2024; Baldassarre, 2025) Therefore, the development of low-cost, low-energy recycling processes for CRMs from secondary sources is in high demand. (Golzar-Ahmadi et al., 2024) Importantly, in the current study, assumptions on element criticality, raw material use and recycling rates were based on European data and regulations. As such, a European energy mix was also used for electricity

assumptions. However, it is expected that the situation will be similar in many other parts of the world and the necessity for TFPV recycling globally will be of high importance in the near future. (Baldassarre, 2025; Akcil et al., 2019)

With the increasing complexity of industrial waste products and wastewater, the separation and recovery of metals using classical pyrometallurgy or hydrometallurgy is becoming increasingly challenging. (İşildar et al., 2018; Sica et al., 2018) As a result, multi-step processes might be required, leading to high chemical and energy consumption and, consequently, a high environmental impact and potential health risks. (Agrawal and Sahu, 2009) In contrast, NF offers a chemical-free way for separation and purification of dissolved metals, as well as for recovery of acid from spent acidic solutions. (Botelho Junior et al., 2023; G. Bargeman, 2021) NF can also be combined with classical hydrometallurgy, and it has been shown that the amount of chemicals required for solvent extraction or precipitation could be considerably reduced after concentration of a waste stream by means of NF. (Hedwig et al., 2022; Zimmermann et al., 2014)

This study has shown that highly stable LbL-NF membranes can be a promising tool for metal recovery in the field of hydrometallurgy. The recovery of In and Ag was demonstrated to be feasible, with Ag showing a lower climate impact than primary production and In potentially benefiting from further optimisation. Thus, apart from a considerable reduction of the precipitating agent (see Section S3), the separation of In and Ag by NF may enable >70 % acid reuse without further treatment. Furthermore, due to high permeability and low TMP, it has been shown that the energy consumption for LbL NF was low compared to commercial NF. (Amrein et al., 2025) However, the long-term stability of LbL membranes has been a major obstacle for the large-scale application of this technology. The results of this study have shown that highly stable LbL-NF membranes can be produced by a combination of PEs and a membrane substrate with high binding strength. While stable LbL configurations for a broad range of mineral acids were found, stability in HCl still leaves room for improvement and should be addressed in future research. This process supports the principles of green membrane design, specifically those promoting low energy demand, extended membrane lifetime and integration into circular flows. (Szekely, 2024) It also contributes to SDGs 7 (Affordable and Clean Energy), 9 (Industry, Innovation and Infrastructure), 12 (Responsible Consumption and Production) and 13 (Climate Action) by reducing climate impact, improving resource recovery and advancing innovation in sustainable materials processing. (United Nations 2015)

5. Conclusion

New-generation thin-film solar cells offer a promising alternative to traditional crystalline silicon solar cells due to their minimal material usage and low-cost processing. Furthermore, since large PCE improvements have been reported, TFPV is expected to play a crucial role in the global energy transition, contributing to climate goals and reducing dependence on fossil fuels. However, their reliance on finite resources such as In and Ag makes efficient recycling essential for long-term sustainability.

This study demonstrated the feasibility of using LbL-NF membranes for the recovery of In and Ag from EOL TFPV. Furthermore, the findings highlight the importance of membrane stability in highly acidic environments, which is a critical factor for industrial-scale applications. A holistic investigation of LbL membrane stability in different inorganic acids has shown that both the type of acid and the LbL membrane composition strongly influence membrane stability. Among the tested membranes, the sPES(PAH/PSS)₄ membrane exhibited the highest stability under acidic conditions, maintaining efficient separation performance over long-term filtration.

Compared with the existing literature, the LCIA of LbL-NF-based recycling of EOL TFPV showed benefits in the GWP values for In and Ag. Additionally, it showed the importance of balancing process yields

with other process optimisation steps, accounting for environmental and economic repercussions. Nevertheless, high-yielding LbL NF can be considered a low-impact recycling step to valorise Ag and In across the entire life cycle of TFPV and help advance the European circular economy. Future research should focus on increasing recovery yields and technology readiness levels in line with LCA insights and recommendations.

CRedit authorship contribution statement

Meret Amrein: Writing – original draft, Visualization, Validation, Methodology, Investigation, Formal analysis, Data curation, Conceptualization. **Karina Rohrer:** Writing – original draft, Visualization, Methodology, Investigation. **Dirk Hengevoss:** Methodology, Investigation. **Tobias Müller:** Investigation. **Bastien Vallat:** Resources, Investigation, Conceptualization. **Dalila Rocco:** Resources, Investigation. **Michael Thomann:** Writing – review & editing. **Frank Nüesch:** Writing – review & editing. **Sebastian Hedwig:** Writing – review & editing. **Markus Lenz:** Writing – review & editing, Conceptualization.

Declaration of competing interest

The authors declare the following financial interests/personal relationships which may be considered as potential competing interests:

Markus Lenz reports financial support was provided by European Union. Markus Lenz reports financial support was provided by Swiss State Secretariat for Education Research and Innovation. If there are other authors, they declare that they have no known competing financial interests or personal relationships that could have appeared to influence the work reported in this paper.

Acknowledgements

Funded by the European Union. Views and opinions expressed are however those of the author(s) only and do not necessarily reflect those of the European Union or RIA. Neither the European Union nor the granting authority can be held responsible for them. NEXUS project has received funding from the European Union's Horizon Europe research and innovation program under grant agreement No 101075330. This work was supported by the Swiss State Secretariat for Education, Research and Innovation (SERI) under Contract No 22.00314. The opinions expressed and arguments employed herein do not necessarily reflect the official views of the Swiss government.

Supplementary materials

Supplementary material associated with this article can be found, in the online version, at [doi:10.1016/j.resconrec.2025.108630](https://doi.org/10.1016/j.resconrec.2025.108630).

Data availability

Data will be made available on request.

References

- Agrawal, A., Sahu, K.K., 2009. An overview of the recovery of acid from spent acidic solutions from steel and electroplating industries. *J. Hazard Mater.* 171 (1), 61–75. <https://doi.org/10.1016/j.jhazmat.2009.06.099>.
- Akcil, A., Agcasulu, I., Swain, B., 2019. Valorization of waste LCD and recovery of critical raw material for circular economy: a review. *Resour. Conserv. Recycl.* 149, 622–637. <https://doi.org/10.1016/j.resconrec.2019.06.031>.
- Amrein, M., Rohrer, K., Hengevoss, D., Jin, H., Snaith, H.J., Thomann, M., Nüesch, F., Lenz, M., 2025. Indium and silver recovery from perovskite thin film solar cell waste by means of nanofiltration. *ACS Sustainable Resour. Manage.* 2 (6), 1087–1095. <https://doi.org/10.1021/acssusresmgmt.5c00109>.
- Amrein, M., Rohrer, K., Hengevoss, D., Jin, H., Snaith, H.J., Thomann, M., Nüesch, F., Lenz, M., 2025. Indium and silver recovery from perovskite thin film solar cell waste by means of nanofiltration. *ACS Sustain. Resour. Manage.* <https://doi.org/10.1021/acssusresmgmt.5c00109>.

- Apergis, I., Apergis, N., 2019. Silver prices and solar energy production. *Environ. Sci. Pollut. Res.* 26 (9), 8525–8532. <https://doi.org/10.1007/s11356-019-04357-1>.
- Bae, H., Kim, Y., 2021. Technologies of lithium recycling from waste lithium ion batteries: a review. *Mater. Adv.* 2 (10), 3234–3250. <https://doi.org/10.1039/D1MA00216C>.
- Baldassarre, B., 2025. Circular Economy for Resource Security in the European Union (EU): case study, research framework, and Future directions. *Ecol. Econ.* 227, 108345. <https://doi.org/10.1016/j.ecolecon.2024.108345>.
- Bargeman, G., 2021a. Recent developments in the preparation of improved nanofiltration membranes for extreme pH conditions. *Sep. Purif. Technol.* 279, 119725. <https://doi.org/10.1016/j.seppur.2021.119725>.
- Bargeman, G., 2021b. Recent developments in the preparation of improved nanofiltration membranes for extreme pH conditions. *Sep. Purif. Technol.* 279, 119725. <https://doi.org/10.1016/j.seppur.2021.119725>.
- Binnemans, K., Jones, P.T., Blanpain, B., Van Gerven, T., Pontikes, Y., 2015. Towards zero-waste valorisation of rare-earth-containing industrial process residues: a critical review. *J. Clean. Prod.* 99, 17–38. <https://doi.org/10.1016/j.jclepro.2015.02.089>.
- Botelho Junior, A.B., Tenório, J.A.S., Espinosa, D.C.R., 2023. Separation of critical metals by membrane technology under a circular economy framework: a review of the State-of-the-art. *Processes* 11 (4), 1256. <https://doi.org/10.3390/pr11041256>.
- Case, C., Beaumont, N., Kirk, D., 2019. Industrial insights into perovskite photovoltaics. *ACS Energy Lett.* 4 (11), 2760–2762. <https://doi.org/10.1021/acsenergylett.9b02105>.
- Chen, J., Xu, S., Tang, C.Y., Hu, B., Tokay, B., He, T., 2023. Stability of layer-by-layer nanofiltration membranes in highly saline streams. *Desalination* 555, 116520. <https://doi.org/10.1016/j.desal.2023.116520>.
- Click, N., Teknetzi, I., Tam, E.P.L., Tao, M., Ebin, B., 2024. Innovative recycling of high purity silver from silicon solar cells by acid leaching and ultrasonication. *Sol. Energy Mater. Sol. Cells* 270, 112834. <https://doi.org/10.1016/j.solmat.2024.112834>.
- de Grooth, J., Haakmeester, B., Wever, C., Potreck, J., de Vos, W.M., Nijmeijer, K., 2015. Long term physical and chemical stability of polyelectrolyte multilayer membranes. *J. Memb. Sci.* 489, 153–159. <https://doi.org/10.1016/j.memsci.2015.04.031>.
- Directorate-General for Internal Market, 2023. Industry, entrepreneurship and SMEs (European Commission). In: Grohol, M., Veeh, C. (Eds.), *Study On the Critical Raw Materials for the EU2023: Final Report*. Publications Office of the European Union.
- Elsosh, M.G., de Vos, W.M., de Grooth, J., Benes, N.E., 2020a. On the long-term pH stability of polyelectrolyte multilayer nanofiltration membranes. *J. Memb. Sci.* 615, 118532. <https://doi.org/10.1016/j.memsci.2020.118532>.
- Elsosh, M.G., de Vos, W.M., de Grooth, J., Benes, N.E., 2020b. On the long-term pH stability of polyelectrolyte multilayer nanofiltration membranes. *J. Memb. Sci.* 615, 118532. <https://doi.org/10.1016/j.memsci.2020.118532>.
- European Commission. Environmental footprint methodology for life cycle assessment, 2023. <https://eplca.jrc.ec.europa.eu>.
- European Innovation Partnership on Raw Materials. Raw Materials Scoreboard 2021. European Platform on LCA | EPLCA, 2025. Environmental footprint methodology for life cycle assessment. accessed. <https://eplca.jrc.ec.europa.eu/>. accessed01-31.
- Farjana, S.H., Huda, N., Mahmud, M.A.P., Lang, C., 2019. Impact analysis of gold silver refining processes through life-cycle assessment. *J. Clean. Prod.* 228, 867–881. <https://doi.org/10.1016/j.jclepro.2019.04.166>.
- Fetting, C., 2020. The European green deal. *ESDN Rep.*
- Free, M.L., 2022. *Hydrometallurgy: Fundamentals and Applications*; The Minerals, Metals & Materials Series. Springer International Publishing: Cham. <https://doi.org/10.1007/978-3-030-88087-3>.
- Fthenakis, V., Athias, C., Blumenthal, A., Kulur, A., Magliozzo, J., Ng, D., 2020. Sustainability evaluation of CdTe PV: an update. *Renew. Sustain. Energy Rev.* 123, 109776. <https://doi.org/10.1016/j.rser.2020.109776>.
- Fu, J., Schlenoff, J.B., 2016. Driving forces for oppositely charged polyanion association in aqueous solutions: enthalpic, entropic, but not electrostatic. *J. Am. Chem. Soc.* 138 (3), 980–990. <https://doi.org/10.1021/jacs.5b11878>.
- Fu, J., Fares, H.M., Schlenoff, J.B., 2017a. Ion-pairing strength in polyelectrolyte complexes. *Macromolecules* 50 (3), 1066–1074. <https://doi.org/10.1021/acs.macromol.6b02445>.
- Fu, J., Fares, H.M., Schlenoff, J.B., 2017b. Ion-pairing strength in polyelectrolyte complexes. *Macromolecules* 50 (3), 1066–1074. <https://doi.org/10.1021/acs.macromol.6b02445>.
- Goldschmidt, J.C., Wagner, L., Pletzcker, R., Friedrich, L., 2021. Technological learning for resource efficient terawatt scale photovoltaics. *Energy Environ. Sci.* 14 (10), 5147–5160. <https://doi.org/10.1039/D1EE02497C>.
- Golzar-Ahmadi, M., Bahaloo-Horeh, N., Pourhossein, F., Norouzi, F., Schoenberger, N., Hintersatz, C., Chakankar, M., Holuszko, M., Kaksonen, A.H., 2024. Pathway to industrial application of heterotrophic organisms in critical metals recycling from E-waste. *Biotechnol. Adv.* 77, 108438. <https://doi.org/10.1016/j.biotechadv.2024.108438>.
- Hawach Scientific, 2024. What is the life expectancy of A membrane filter? <https://www.hawachmembrane.com/what-is-the-life-expectancy-of-a-membrane-filter/> accessed 2025-01-31.
- Hedwig, S., Yagmurulu, B., Huang, D., von Arx, O., Dittrich, C., Constable, E.C., Friedrich, B., Lenz, M., 2022. Nanofiltration-enhanced solvent extraction of scandium from TiO₂ acid waste. *ACS Sustain. Chem. Eng.* 10 (18), 6063–6071. <https://doi.org/10.1021/acssuschemeng.2c01056>.
- Hedwig, S., Yagmurulu, B., Peters, E.M., Misev, V., Hengevoss, D., Dittrich, C., Forsberg, K., Constable, E.C., Lenz, M., 2023a. From trace to pure: pilot-scale scandium recovery from TiO₂ acid waste. *ACS Sustain. Chem. Eng.* 11 (15), 5883–5894. <https://doi.org/10.1021/acssuschemeng.2c06979>.
- Hedwig, S., Yagmurulu, B., Peters, E.M., Misev, V., Hengevoss, D., Dittrich, C., Forsberg, K., Constable, E.C., Lenz, M., 2023b. From trace to pure: pilot-scale scandium recovery from TiO₂ acid waste. *ACS Sustain. Chem. Eng.* 11 (15), 5883–5894. <https://doi.org/10.1021/acssuschemeng.2c06979>.
- ISO, 2025. 14040:2006(en), Environmental management — Life cycle assessment — Principles and framework. accessed. <https://www.iso.org/obp/ui/#iso:std:iso:14040:ed-2:v1:en>. accessed02-03.
- Intergovernmental Panel On Climate Change (Ippc), 2023. Climate Change 2021 – The Physical Science Basis: Working Group I Contribution to the Sixth Assessment Report of the Intergovernmental Panel on Climate Change, 1st ed. Cambridge University Press. <https://doi.org/10.1017/9781009157896>.
- İşıldar, A., Rene, E.R., van Hullebusch, E.D., Lens, P.N.L., 2018. Electronic waste as a secondary source of critical metals: management and recovery technologies. *Resour. Conserv. Recycl.* 135, 296–312. <https://doi.org/10.1016/j.resconrec.2017.07.031>.
- Jonkers, W.A., Cornelissen, E.R., de Vos, W.M., 2023. Hollow Fiber nanofiltration: from lab-scale research to full-scale applications. *J. Memb. Sci.* 669, 121234. <https://doi.org/10.1016/j.memsci.2022.121234>.
- Lasisi, K.H., Tao, B., Shao, S., Liu, M., Zhang, K., 2025. Sustainable spray coating fabrication of acid-resistant polyamine nanofiltration membrane to separate heavy metal ions and treat acid wastewater. *J. Memb. Sci.* 724, 123989. <https://doi.org/10.1016/j.memsci.2025.123989>.
- Lee, J., Shin, Y., Boo, C., Hong, S., 2023. Performance, limitation, and opportunities of acid-resistant nanofiltration membranes for industrial wastewater treatment. *J. Memb. Sci.* 666, 121142. <https://doi.org/10.1016/j.memsci.2022.121142>.
- Li, N., Niu, X., Chen, Q., Zhou, H., 2020. Towards commercialization: the operational stability of perovskite solar cells. *Chem. Soc. Rev.* 49 (22), 8235–8286. <https://doi.org/10.1039/D0CS00573H>.
- Lundaev, V., Solomon, A.A., Le, T., Lohrmann, A., Breyer, C., 2023. Review of critical materials for the energy transition, an analysis of global resources and production databases and the State of material circularity. *Min. Eng.* 203, 108282. <https://doi.org/10.1016/j.mineng.2023.108282>.
- Mejías, O., Parbhakar-Fox, A., Jackson, L., Valenta, R., Townley, B., 2023. Indium in ore deposits and mine waste environments: geochemistry, mineralogy, and opportunities for recovery. *J. Geochem. Explor.* 255, 107312. <https://doi.org/10.1016/j.gexplo.2023.107312>.
- Newman, P.; Meader, N.; Klapwijk, P.; Liang, J.; Chou, E.; Gao, Y.; Barot, H.; Furuno, A.; Rey, F.; Yau, S.; Kong, H.; Belge, M.; Diwe, A.; Kavalis, N.; Swarts, W.; Webb, A.; Munro, D.; Ryan, P.; Sheth, C.; Küçükmiroglu, Ç.; Bedford, M.; Gao, J.; Zarate, C.; Tomlinson, S. Metals focus World silver Survey 202. 2021.
- Nuss, P., Eckelman, M.J., 2014. Life cycle assessment of metals: a scientific synthesis. *PLoS One* 9 (7), e101298. <https://doi.org/10.1371/journal.pone.0101298>.
- Oliveira, L.S.S.D., Lima, M.T.W.D.C., Yamane, L., Siman, R.R., 2020. Silver recovery from end-of-life photovoltaic panels. *Detritus* (10), 62–74. <https://doi.org/10.31025/2611-4135/2020.13939>.
- Overview and key findings – World Energy Investment, 2024. 2024 – Analysis. IEA. accessed. <https://www.iea.org/reports/world-energy-investment-2024/overview-and-key-findings>. accessed-07-31.
- O’Neal, J.T., Dai, E.Y., Zhang, Y., Clark, K.B., Wilcox, K.G., George, I.M., Ramasamy, N. E., Enriquez, D., Batys, P., Sammalkorpi, M., Lutkenhaus, J.L., 2018. QCM-D investigation of swelling behavior of layer-by-layer thin films upon exposure to monovalent ions. *Langmuir* 34 (3), 999–1009. <https://doi.org/10.1021/acs.langmuir.7b02836>.
- PDF, 2022. accessed. <https://web.archive.org/web/20211203232214id/http://publications.rwth-aachen.de/record/782953/files/782953.pdf>. accessed-07-28.
- Paltrinieri, L., Remmen, K., Müller, B., Chu, L., Köser, J., Wintgens, T., Wessling, M., de Smet, L.C.P.M., Sudhölter, E.J.R., 2019. Improved phosphoric acid recovery from sewage sludge ash using layer-by-layer modified membranes. *J. Memb. Sci.* 587, 117162. <https://doi.org/10.1016/j.memsci.2019.06.002>.
- Park, H.B., Kamcev, J., Robeson, L.M., Elimelech, M., Freeman, B.D., 2017. Maximizing the right stuff: the trade-off between membrane permeability and selectivity. *Science* 356 (6343), eaab0530. <https://doi.org/10.1126/science.aab0530>.
- Park, J.R., Lee, C.G., Swain, B., 2023. Beneficiation and classification of ITO concentrate from waste LCD panel for industrial-scale indium extraction. *Environ. Sci. Pollut. Res.* 30 (39), 90209–90222. <https://doi.org/10.1007/s11356-023-26106-1>.
- Pommeret, A., Ricci, F., Schubert, K., 2022. Critical raw materials for the energy transition. *Eur. Econ. Rev.* 141, 103991. <https://doi.org/10.1016/j.euroecorev.2021.103991>.
- Remmen, K., Schäfer, R., Hedwig, S., Wintgens, T., Wessling, M., Lenz, M., 2019a. Layer-by-Layer membrane modification allows scandium recovery by nanofiltration. *Environ. Sci.: Water Res. Technol.* 5 (10), 1683–1688. <https://doi.org/10.1039/C9EW00509A>.
- Remmen, K., Müller, B., Köser, J., Wessling, M., Wintgens, T., 2019b. Phosphorus recovery in an acidic environment using layer-by-layer modified membranes. *J. Memb. Sci.* 582, 254–263. <https://doi.org/10.1016/j.memsci.2019.03.023>.
- Remmen, K., Müller, B., Köser, J., Wessling, M., Wintgens, T., 2020. Assessment of layer-by-layer modified nanofiltration membrane stability in phosphoric acid. *Membr. (Basel)* 10 (4), 61. <https://doi.org/10.3390/membranes10040061>.
- Renewables, 2024. Pdf. <https://iea.blob.core.windows.net/assets/17033b62-07a5-4144-8dd0-651cddb6caa24/Renewables2024.pdf>. accessed 2025-02-10.
- Rizos, V., Righetti, E., Kassab, A., 2024. Understanding the barriers to recycling critical raw materials for the energy transition: the case of rare earth permanent magnets. *Energy Rep.* 12, 1673–1682. <https://doi.org/10.1016/j.egy.2024.07.022>.
- Rushton, A., Ward, A.S., Holdich, R.G., 1996. Solid-Liquid Filtration and Separation Technology, 1st ed. Wiley. <https://doi.org/10.1002/9783527614974>.
- Savvilitidou, V., Gidarakos, E., 2020. Pre-concentration and recovery of silver and indium from crystalline silicon and copper indium selenide photovoltaic panels. *J. Clean. Prod.* 250, 119440. <https://doi.org/10.1016/j.jclepro.2019.119440>.

- Scheepers, D., Borneman, Z., Nijmeijer, K., 2024. Nanofiltration membrane performance of layer-by-layer membranes with different polyelectrolyte concentrations. *Desalination* 574, 117246. <https://doi.org/10.1016/j.desal.2023.117246>.
- Schmidt, F., Schäffer, A., Lenz, M., 2019. Renewable energy from finite resources: example of emerging photovoltaics. *Chim. (Aarau)* 73 (11). <https://doi.org/10.2533/chimia.2019.874>, 874–874.
- Sica, D., Malandrino, O., Supino, S., Testa, M., Lucchetti, M.C., 2018. Management of end-of-life photovoltaic panels as a step towards a circular economy. *Renew. Sustain. Energy Rev.* 82, 2934–2945. <https://doi.org/10.1016/j.rser.2017.10.039>.
- Sinha, P., Raju, S., Drozdziak, K., Wade, A., 2018. Life cycle management and recycling of PV systems., ECS Meeting Abstracts, MA2018-02(17):729-729. [doi:10.1149/MA2018-02/17/729](https://doi.org/10.1149/MA2018-02/17/729).
- Sustainability in Membrane Technology, 2025. Membrane recycling and fabrication using recycled waste. accessed. <https://www.mdpi.com/2077-0375/14/2/52>. accessed-02-16.
- Sverdrup, H.U., van Allen, O., Haraldsson, H.V., 2024. Modeling indium extraction, supply, price, use and recycling 1930–2200 using the WORLD7 model: implication for the imaginaries of sustainable Europe 2050. *Nat. Resour. Res.* 33 (2), 539–570. <https://doi.org/10.1007/s11053-023-10296-z>.
- Szekely, G., Jimenez-Solomon, M.F., Marchetti, P., Kim, J.F., Livingston, A.G., 2014. Sustainability assessment of organic solvent nanofiltration: from fabrication to application. *Green. Chem.* 16 (10), 4440–4473. <https://doi.org/10.1039/C4GC00701H>.
- Szekely, G., 2024. The 12 principles of green membrane materials and processes for realizing the United Nations' Sustainable Development Goals. *RSC Sustain.* 2 (4), 871–880. <https://doi.org/10.1039/D4SU00027G>.
- United Nations, 2015. Transforming our world: the 2030 Agenda for Sustainable Development. <https://sdgs.un.org/2030agenda>.
- Wagner, L.; Suo, J.; Yang, B.; Bogachuk, D.; Gervais, E.; Pietzcker, R.; Gassmann, A.; Goldschmidt, J.C. The resource demand of terawatt-scale perovskite tandem photovoltaics. 2023. <https://doi.org/10.2139/ssrn.4493241>.
- Yaroshchuk, A., Bruening, M.L., Zholkovskiy, E., 2019. Modelling nanofiltration of electrolyte solutions. *Adv. Colloid. Interface Sci.* 268, 39–63. <https://doi.org/10.1016/j.cis.2019.03.004>.
- Yin, Y., Li, C., Ng, D.Y.F., Wang, R., 2025. Highly permeable acid-resistant polyamine hollow Fiber nanofiltration membrane fabricated by secondary interfacial polymerization reactions. *J. Memb. Sci.* 716, 123502. <https://doi.org/10.1016/j.memsci.2024.123502>.
- Yu, L., Moriguchi, Y., Nakatani, J., Zhang, Q., Li, F., He, W., Li, G., 2019. Environmental Impact assessment on the recycling of waste LCD panels. *ACS Sustain. Chem. Eng.* 7 (6), 6360–6368. <https://doi.org/10.1021/acssuschemeng.9b00119>.
- Yu, Y., Bai, X., Li, S., Shi, J., Wang, L., Xi, F., Ma, W., Deng, R., 2023. Review of silicon recovery in the photovoltaic industry. *Curr. Opin. Green Sustain. Chem.* 44, 100870. <https://doi.org/10.1016/j.cogsc.2023.100870>.
- Yu, M., Ren, T.-X., Jin, X.-G., Tang, X., Tang, M.-M., Ma, X.-H., Xu, Z.-L., 2024. Theoretical and experimental research of polyelectrolyte multilayer membrane prepared by layer by layer self-assembly. *Desalination* 580, 117561. <https://doi.org/10.1016/j.desal.2024.117561>.
- Zhang, Y., Kim, M., Wang, L., Verlinden, P., Hallam, B., 2021. Design considerations for multi-terawatt scale manufacturing of existing and future photovoltaic technologies: challenges and opportunities related to silver, indium and bismuth consumption. *Energy Environ. Sci.* 14 (11), 5587–5610. <https://doi.org/10.1039/D1EE01814K>.
- Zheng, K., Benedetti, M.F., van Hullebusch, E.D., 2023. Recovery technologies for indium, gallium, and germanium from end-of-life products (Electronic Waste) – A review. *J. Environ. Manage* 347, 119043. <https://doi.org/10.1016/j.jenvman.2023.119043>.
- Zimmermann, Y.-S., Niewersch, C., Lenz, M., Kül, Z.Z., Corvini, P.F.-X., Schäffer, A., Wintgens, T., 2014. Recycling of indium from CIGS photovoltaic cells: potential of combining acid-resistant nanofiltration with liquid–Liquid extraction. *Environ. Sci. Technol.* 48 (22), 13412–13418. <https://doi.org/10.1021/es502695k>.